# Shape and size of the current head in creeping flows

B. M. Marino, L. P. Thomas, and R. Gratton
*Instituto de Física Arroyo Seco, Facultad de Ciencias Exactas, Universidad Nacional del Centro, Pinto 399, 7000 Tandil, Argentina*
(Received 17 October 1996)

We investigate the shape and the size of the current head formed when a viscous liquid driven by gravity spreads on a horizontal smooth substrate. A characteristic roll-shaped current head is observed during the experiments, which evolves towards a wedgelike shape when the (decreasing) capillary number Ca goes below the unity. The lower part of the advancing roll observed when $\mathrm{Ca}\gg 1$ may be described as half a cusped entrance of the free liquid surface, centered on the spreading surface. The size of the roll structure during this stage is proportional to the square of the front velocity which, in turn, is determined by the global dynamics of the flow. [S1063-651X(97)10304-X]

PACS number(s): 47.15.Gf, 47.10.+g

## I. INTRODUCTION

When a thick liquid layer spreads on a dry substrate and surface forces are small, the rim looks like an advancing roll whose leading nose precedes the underlying contact line. This work concerns the shape of this roll-like head in creeping flows, where also inertial forces are negligible. By defining the capillary number $\mathrm{Ca}=\rho\nu u_f/\gamma$ and the Reynold number $\mathrm{Re}=x_f u_f/\nu$ ($\nu$ and $\rho$ are the kinematic viscosity and density of the liquid, $\gamma$ is the liquid-air surface tension, $x_f$ is the extent of the current in the direction of the advance or *front position*, and $u_f=dx_f/dt$ is the rate of advance of the leading point), the above conditions are expressed as $\mathrm{Re}\ll 1$ and $\mathrm{Ca}\gg 1$. In a previous work we studied large axisymmetric spreadings of wetting liquids on a smooth substrate [1], which initially satisfied both conditions. After the flow release, the silhouette of the head tends to an invariant roll-like shape (asymptotic shape), whose size decreases according to a simple power law dependence on $u_f$. Because of the constancy of the volume, $u_f$ and then Ca decrease quickly as the flow proceeds. When $x_f$ takes a critical value (corresponding to $\mathrm{Ca}\approx 1.7$), the profile changes drastically to a wedgelike shape. Since that work was mainly addressed to point out the existence of this transition and its effects on the global dynamics, a deeper study of the previous stage characterized by large Ca was not carried out. Furthermore, the current was observed laterally, so that the shape of the leading roll near the contact line and the position of this line were affected by an uncertainty which made a precise description of the lower region of the head profile impossible. A numerical simulation of a pure gravitational creeping flow in plane geometry, based on the contour elements method, led substantially to the same asymptotic roll-like shape of the current head [2]. Some works [3–6] concerning the value of the dynamic contact angle show that it is close to 180° for $\mathrm{Ca}\gtrsim 1$, in agreement with the above results. Nevertheless, while there is a sound theoretical background on wedge-shaped heads ($\mathrm{Ca}\ll 1$) [5,7–11], there is a lack of analytical models for the roll-shaped heads leading currents when $\mathrm{Ca}\gg 1$.

On the other hand, the formation of cusped entrances where the free surface is sucked into the fluid has been reported for a variety of Stokes flows. Known examples arise when a viscous liquid is forced to move by two parallel counterrotating cylinders, provided $\mathrm{Ca}>2.5$ [12,13], or in the lowest end of an air drop rising in a liquid [14,15]. For zero surface tension ($\mathrm{Ca}\to\infty$), Joseph *et al.* [12] found a solution by considering the velocity field near the cusp vertex as a small perturbation of a uniform stream parallel to the tangent at the cusp. If $\zeta$ is the distance between the free surface and the plane of symmetry and $\xi$ is the Cartesian coordinate orthogonal to the cusp line in the same plane, measured from the vertex, the contour of the cusp is given by $\zeta\sim\xi^{3/2}$ for $\zeta\ll\xi$. Jeong and Moffatt [13] solved a model problem related to the two-cylinder experiment by using complex analysis and conformal mapping techniques. For Ca finite, the solution is regular with a stagnation point at the cusp edge. However, the radius of curvature, $R$, at this point is very small when Ca is of the order of unity or greater. For $\mathrm{Ca}\gtrsim 1$, the free surface contour at distances larger than $R$ from the cusp line is given by $\zeta=c\xi^{3/2}$, with $c$ of the order of unity, and is independent of surface tension. This law holds for Newtonian and some special non-Newtonian liquids, and can be obtained on the basis of simple geometrical considerations [16].

The object of the present paper is to provide an improved experimental description of the asymptotic roll-shaped head for plane viscous gravity currents with $\mathrm{Ca}>1$. The results substantiate that the lower region of the roll may be considered as one-half of a cusped entrance edged by the contact line, whose plane of symmetry coincides with the spreading surface. We report measurements of the positions of the leading point of the current $x_f(t)$ and of the contact line $x_{\mathrm{cl}}(t)$, and by an independent refractive profilometric technique we obtain both the liquid contour $h(x)$ and its spatial derivative $\partial h/\partial x$ throughout the entire flow with high accuracy. We observe the same asymptotic roll-like shape reported by Marino *et al.* [1] notwithstanding the different symmetries and initial configurations involved. However, thanks to the improved experimental technique used, we are able to show that the contour of the lower part of the roll is described by the curve $\zeta\sim\xi^{3/2}$, where $\zeta$ is the height with respect to the spreading surface and $\xi$ is proportional to $x-x_{\mathrm{cl}}$. For the regime studied, this suggests that the specific surface effects associated with the spreading surface are negligible on a macroscopic scale, and therefore that the mathematical prob-

 

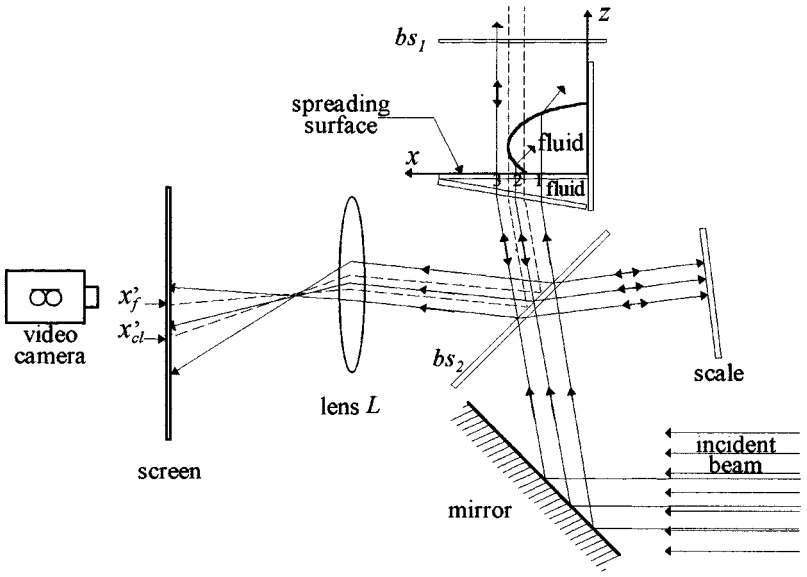


FIG. 1. Experimental setup for measuring $x_f(t)$ and $x_{cl}(t)$. The beam splitters $bs_1$ and $bs_2$ reflect about 16% and 50%, respectively. The lens $L$ forms the image of the spreading surface ($z=0$) on the screen.

lem for cusped entrances solved by Joseph *et al.* [12] and Jeong and Moffatt [13] seems quite adequate to model the head of a creeping flow near the contact line. Finally, we investigate the limits of this asymptotic stage, which in our case is restricted in time because Ca approaches unity as the spreadings proceed. In particular, the basis of the roll is progressively perturbed so that the entrance becomes less pronounced and the cusp analogy is no longer valid.

## II. EXPERIMENTAL PROCEDURE

We prepare an experimental setup addressed to the study of the leading zone of the current. The liquid is contained in a rectangular glass tray (width 0.30 m, length 0.10 m, height 0.10 m) which can rotate around a horizontal axis near the rear end; the large width to length ratio of the tray ensures that the sidewalls do not affect the flow in the central region where, therefore, all the magnitudes are virtually independent of the transverse coordinate. After cleaning carefully the spreading surface with hexane and alcohol, we tilt the tray an angle $\alpha$ with respect to the horizontal and introduce the liquid. When the liquid surface becomes flat, we let the tray fall to the horizontal position (determined by stops) and the experiment starts. Initially ($t=0$), the liquid forms a triangular prism which covers a length $x_0$ of the horizontal substrate ($h=0$) and is limited by a vertical rear wall at $x=0$ with the free surface inclined by the angle $\alpha$ respect to the horizontal spreading surface. A remarkable property of this initial configuration is that the liquid edge remains at rest for a finite time $t_w$ (*waiting time*) before moving [17–20]; therefore, the earlier times of the liquid spreading beyond $x_0$ correspond to a relatively advanced stage of the flow evolution, little affected by the release procedure. The spreading surface is horizontal within $10^{-4}$ rad. The fluid used is a silicone oil (polydimethylsiloxane) of high viscosity ($\nu \cong 10^3$ cm$^2$ s$^{-1}$, $\rho=0.975$ g cm$^{-3}$, refraction index $\eta=1.4$); departures from a Newtonian behavior are not relevant for the shear rates of the experiments ($\leqslant 1$ s$^{-1}$) [1,21,22]. The condition that inertial forces be small (Re$\ll 1$) limits the liquid volume [1,20,23]. On the other hand, both the average thickness $\langle h(t)\rangle$ and $x_0$ are limited from below by the conditions $B=(x_0/a)^2 \gg 1$ and $\langle h/a\rangle^2 \gg 1$ [where $B$ is the Bond number and $a=(\gamma/\rho g)^{1/2}$ is the capillary length], which ensure that the surface tension effects on the bulk are small and that there is a stage with Ca$\gg 1$ [1,20,23].

The height distribution is obtained by using an accurate profilometer, developed by Thomas *et al.* [24]. This technique provides the distributions of the coordinate $x$ of the surface and of the $\partial x/\partial h$ as function of $h$ for $-85° \leqslant \theta \leqslant 85°$, where $\theta$ is the angle formed by the normal to the free surface and the $x$ axis. The vanishing of $\partial x/\partial h$

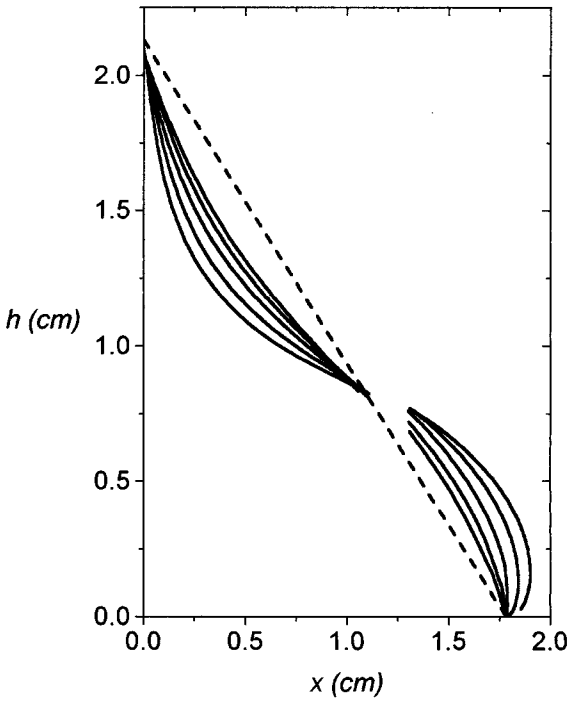


FIG. 2. Sequence of the height profiles of the current for $\alpha=50°$, $x_0=1.783$ cm, $t_w=3.2$ s, and $t=0.5t_w$, $0.75t_w$, $t_w$, $1.5t_w$, and $2t_w$. The dashed line corresponds to the initial profile ($t=0$).

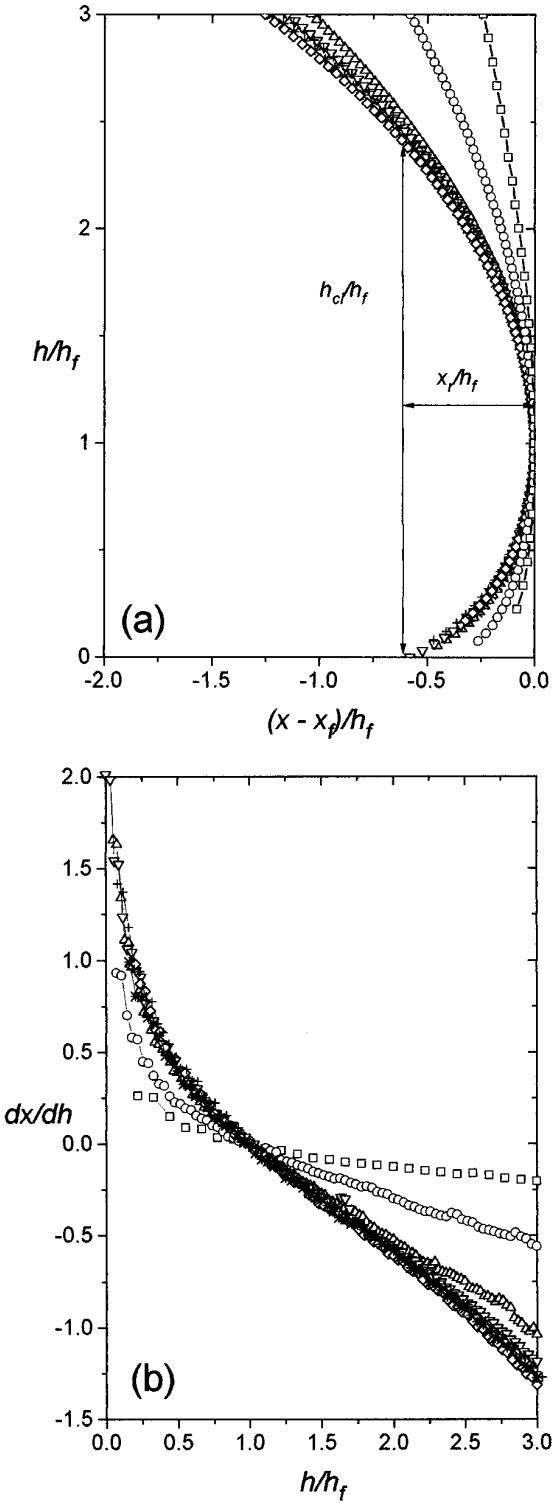


FIG. 3. Dimensionless height (a) and slope distributions (b) near the front for $\alpha = 55°$ and $x_0 = 3.868$ cm, for $t = 1.3t_w$ (□), $t = 2t_w$ (○), $t = 4t_w$ (△), $t = 8t_w$ (∇), $t = 12t_w$ (◇), $t = 16tw$ (+), and $t = 20t_w$ (*). They show the evolution of the roll-shaped current head up to the asymptotic stage.

gives the height $h_f$ of the liquid at $x_f$ with an uncertainty less than $10^{-2}$ cm.

Simultaneously, we measure $x_f(t)$ and $x_{\mathrm{cl}}(t)$ by using the optical system depicted in Fig. 1. A parallel light beam (5 cm diameter) impinges orthogonally from below on the tray.

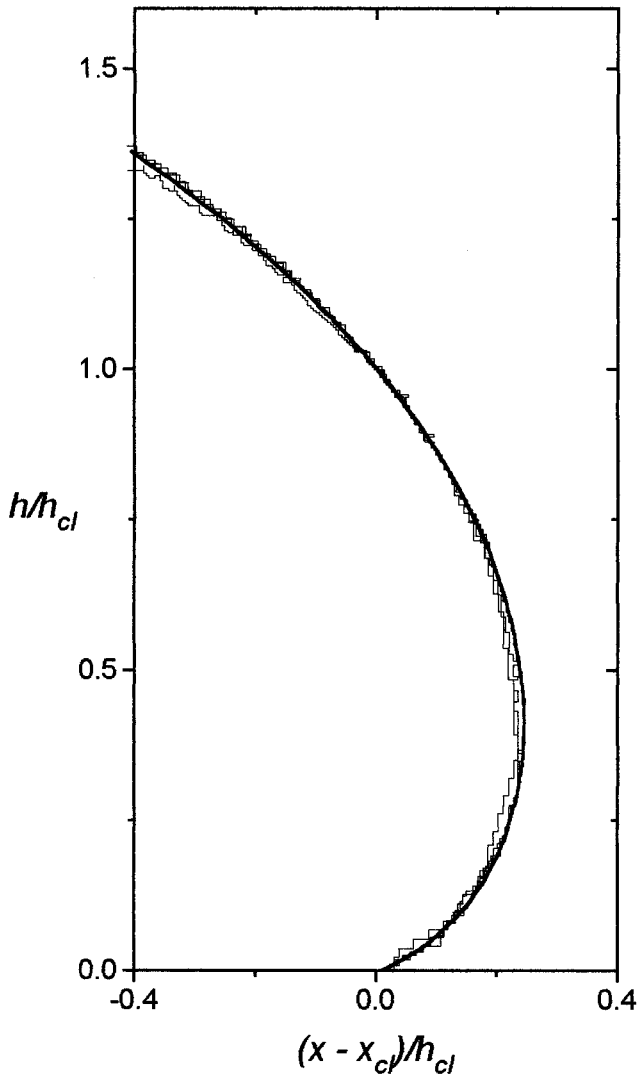


FIG. 4. Comparison between one of the asymptotic head profile of Fig. 3 ($t = 8t_w$, thick line) and three asymptotic head profiles obtained during the axysimmetric spreading of 1504 $cm^3$ of a highly viscous PDMS.

Thanks to the beam splitter $bs_2$ and the lens $L$, we obtain an image of the spreading surface formed by the backward reflected rays. The light reflected by the lower face of the substrate is eliminated by adding a prism-shaped cell filled with the same liquid used in the experiments. The beam splitter $bs_1$, carefully oriented parallel to the spreading surface, ensures a strong ($\approx 16\%$) backward reflection of the rays which pass beyond the nose of the current. Therefore, three well-defined regions with different luminosities appear on the screen. Region 1, corresponding to the wetted part of the spreading surface, looks dark since the reflection is very low there ($\approx 0.17\%$), and neither the liquid-air surface nor the beam splitter $bs_1$ contribute to the image because rays crossing the liquid are strongly deviated. Then, an intermediate narrow region (2) follows; it corresponds to the part of the spreading surface not yet wetted just below the head of the current, where the main contribution is due to the light reflected at the dry upper face of the substrate ($\approx 4.3\%$). Finally, a third zone (3) beyond the nose appears strongly illuminated because of the contribution of $bs_1$. By means of a

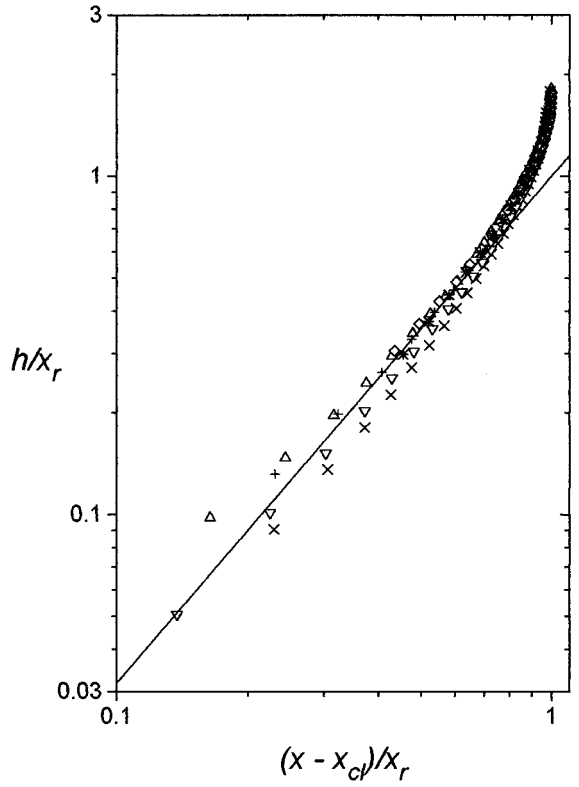


FIG. 5. Log-log representation of the roll contours below the nose for the same cases of Fig. 3 ($7 \leqslant \mathrm{Ca} \leqslant 19$). The solid line is the curve $h_f/x_r=[(x-x_{\mathrm{cl}})/x_r]^{3/2}$.

video camera, we record the image so obtained, superimposed with the image of a calibrated scale conveniently placed behind $\mathrm{bs}_2$. After digitizing with a frame grabber and processing by standard software, the positions of the borders among the differently illuminated regions give $x_f$ and $x_{\mathrm{cl}}$ with an accuracy of about $5\times10^{-3}$ cm.

## III. RESULTS

We carry out a series of experiments with different initial wedge angles ($15° \leqslant \alpha \leqslant 70°$, measured by a goniometer with a $5'$ precision) and initial current lengths (1 cm $<x_0<4$ cm). As reported separately [23], we observe first a redistribution of the fluid behind the front at rest. At $t=t_w$ the slope of the free surface becomes vertical at the front which starts to move while the current head develops a roll-like form with a prominent nose overhanging the contact line. As an example, a sequence of height distributions across the whole flow is shown in Fig. 2. The gap in a small intermediate region ($x\approx1.25$ cm) is due to the fact that the profilometric technique used gives an uncertainty greater than 2% there [24]. From now on we shall refer only to the leading region.

In all the experiments the current is headed by a roll-like configuration since the beginning of the front motion. First, the shape of the roll changes considerably and its size increases quickly up to a maximum; during this stage (not studied here) the evolution of the characteristic parameters of the head and their relation with the rate of advance of the nose depend on the initial conditions. Then, for $x_f \gtrsim 1.6x_0$

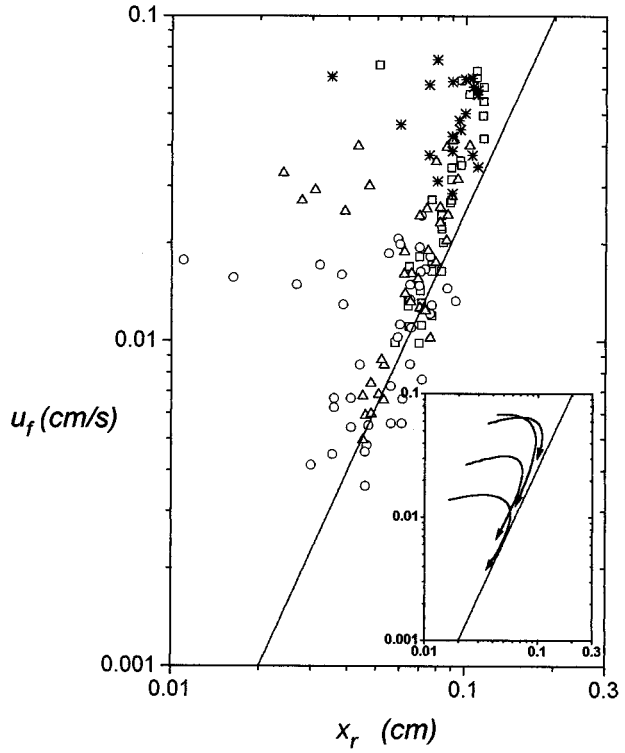


FIG. 6. Front velocity as function of $x_r$ for the cases $\alpha=55°$ and $x_0=3.53$ cm (*), $\alpha=52.5°$ and $x_0=2.01$ cm (□), $\alpha=45°$ and $x_0=1.91$ cm (△), and $\alpha=29.8°$ and $x_0=2.3$ cm (○). In spite of the considerable dispersion, due to the fact that the velocity is obtained from measurements of positions, the experimental points fit well the line $v_f=2.5x_r^2$ during the asymptotic stage. The inset shows the qualitative behavior for the cases reported; the arrows indicate the time evolution.

and provided that Ca is still considerably larger than unity, this configuration asymptotes an invariant shape. This behavior is illustrated in Figs. 3(a) and 3(b) where we reproduce a typical sequence of early head profiles and distributions of $\partial x/\partial h$ scaled in terms of the height $h_f$ of the leading point. All these profiles correspond to high capillary numbers ($\mathrm{Ca}>4.5$). The trend towards an invariant shape is clearly seen specially in the curves of Fig. 3(b). As we shall show later, once the asymptotic shape is attained, the size of the roll is related to the rate of advance of the front and decreases as the spreading progresses. In Fig. 4 we compare (in units of the thickness just over the contact line $h_{\mathrm{cl}}$) one of the asymptotic head profiles obtained in this work with three asymptotic head profiles for an axial viscous gravity current starting from a completely different initial condition [1]. The later profiles were shifted in the $x$ direction and superposed by means of an appropriate scaling (some percent, the same for both axis); this procedure is needed because the respective contact line positions were not well determined (within 3%). Clearly, the asymptotic shape is the same for both cases, thus suggesting that it is independent of the flow symmetry and of the initial conditions. Figure 5 shows the experimental points corresponding to the parts of the profiles between $x_{\mathrm{cl}}$ and $x_f$ for the advanced (asymptotic) cases of Fig. 3. We observe that they follow the power law $h\sim(x-x_{\mathrm{cl}})^{3/2}$, even at distances of the order of $0.7x_r$ from the contact line, with $x_r=x_f-x_{\mathrm{cl}}$.

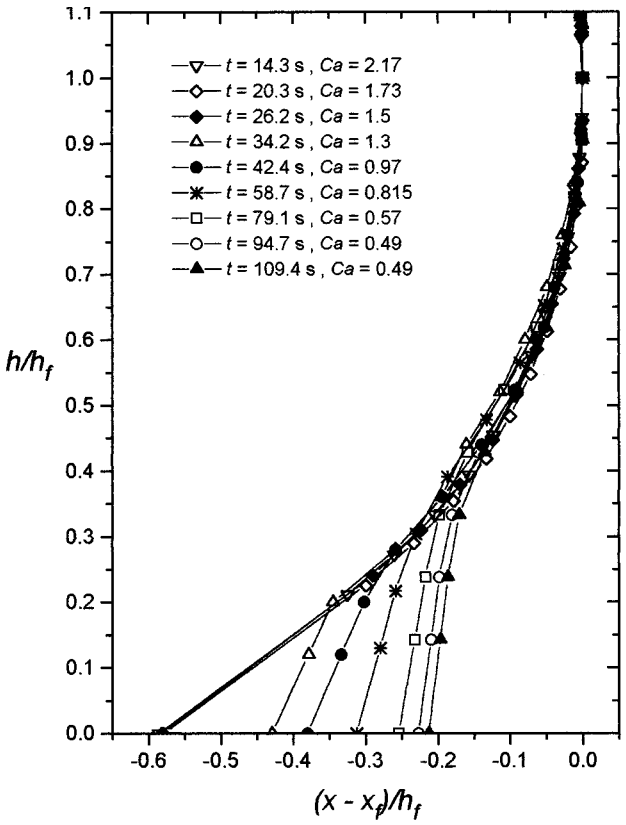


FIG. 7. After a brief asymptotic evolution, the roll-shaped nose evolves to a wedgelike shape when Ca is near unity or less. This figure shows an enlarged view of the head contours near the contact line for the experiment with $\alpha=55°$, $x_0=1.753$ cm.

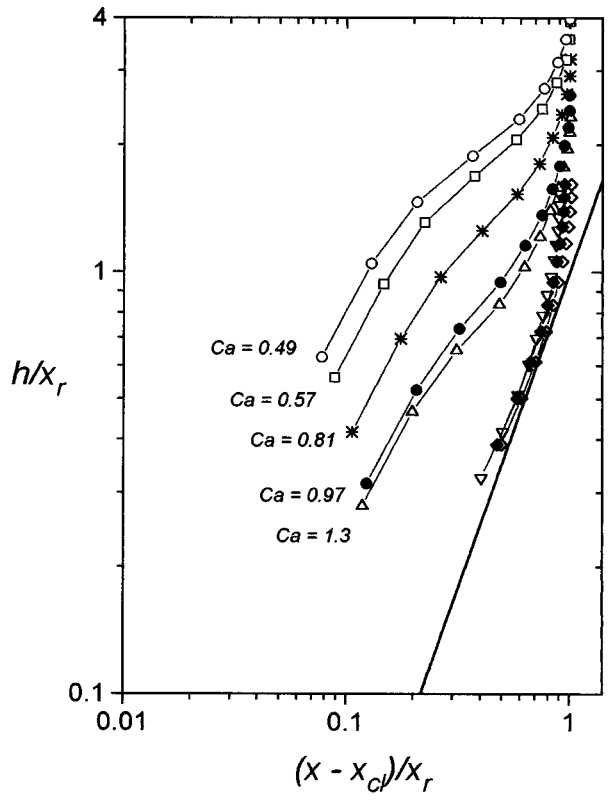


FIG. 8. Log-log representation of the roll contours below the nose for the same cases of Fig. 7. Note the departures from the $[(x-x_{\rm cl})/x_r]^{3/2}$ law (cusped entrances) for $\mathrm{Ca}\leqslant 1$.

It is interesting to analyze the evolution of the roll in terms of the geometric parameters $h_f(t)$, $x_r(t)$, and the velocities $u_{\rm cl}$, $u_f$ (see Fig. 6). Just after the liquid front starts to move, $h_f(t)$ and $x_r(t)$ increase quickly up to a well-defined maximum while $u_f$ is about constant and $u_{\rm cl}$ approaches $u_f$; this moment may be considered as the beginning of the asymptotic stage, characterized by a slow decrease of $h_f$ and of $x_r$, and by the approximate equality of $u_{\rm cl}$ and $u_f$. The ratios $h_f/x_r$ and $h_{\rm cl}/x_r$ take the constant values 1.7 and 4.06, respectively; the last value differs by only 1.5% from that obtained previously for axial spreadings [1]. On the other hand, $u_f$ (or $u_{\rm cl}$) is proportional to $x_r^2$; we shall discuss this result in Sec. IV. Finally, $x_f$ is proportional to $t^{0.2}$ (or $t^{0.125}$ for axial symmetry) according to a known result [1,25] obtained by applying the lubrication approximation, which holds for the bulk of the flow but not in the leading region. The behavior of the leading region continues on until $\mathrm{Ca}\approx 1$, when the head profile starts to change to a wedgelike head shape. As described previously [1], the ratio $h_{\rm cl}/x_r$ (and $h_f/x_r$) increases while $u_f$ slightly decreases. The profilometric technique allows to show clearly how this change begins near the contact line (see Fig. 7), in agreement with a decrease of the contact angle to values considerably lower than 180° when Ca is about the unity or less [3,6].

## IV. DISCUSSION AND CONCLUDING REMARKS

The previous results concerning the asymptotic stage suggest an interpretation based on a few simple assumptions.

(a) The rate of advance $v_f$ of the front is determined by the global dynamics, in turn governed by the lubrication approximation as far as the average liquid thickness is much less than $x_f$ and surface effects may be neglected in the bulk $(B\gg 1)$.

(b) The size of the roll structure which leads the current is determined by the front velocity.

(c) The lower region of the roll can be seen as half a cusped entrance in the free surface of a viscous fluid.

In fact, the global flow imposes a given velocity profile near the front which is a boundary condition for the flow in the head. As the flow proceeds, the magnitude of the velocity changes but not the shape of the velocity profile. Thus, as $\mathrm{Re}\ll 1$, the flow in the head region follows the magnitude changes by adjusting only its size. A similar head shape should be obtained if the same kind of velocity profile near the head would be imposed by moving the rear wall, by injecting fluid at $x=0$, etc.

Item (b) may be clarified by means of the following simple heuristic argument. In the leading region, the rate of the variation of the potential energy of the head is proportional to $(\rho h_f x_r) g u_h$, where $u_h\approx u_f$ is the vertical component of the flow velocity at $h_f$. Then, as the potential energy should be completely dissipated by viscosity,

$$\rho g h_f x_r u_f=\lambda\rho\nu\frac{u_f^2}{h_f^2}h_f x_r, \tag{1}$$

where $\lambda$ is a coefficient of proportionality. Then,

$$u_f = \lambda \frac{g}{\nu} h_f^2 . \qquad (2)$$

As in the asymptotic regime $h_f \sim x_r$, we also have $u_f \sim x_r^2$. According to Fig. 6, $\lambda = 0.18$.

The contact angle is about 180° provided Ca$>1$ and the flow is not macroscopically affected in the head region by the presence of the rigid spreading surface. Therefore, the theoretical analyses performed by Joseph *et al.* [12] and Jeong and Moffatt [13] are good approximations in the neighborhood of the contact line. Thus, $h/x_r = [(x - x_{cl})/x_r]^{3/2}$ and others characteristic features of the flow may certainly be obtained from these solutions.

As Ca decreases below unity, the shape of the head (Fig. 7) displays a change, leading to an evolution towards a wedge-shaped profile. This evolution is qualitatively analogous to the change of the free surface shape in the experiments of rotating cylinders quoted in Sec. I. In the present experiments the change becomes appreciable for Ca$\approx 1.3$, which compares well with the values reported by Joseph *et al.* [12] for the disappearance of the cusp configuration. It is interesting to note that the validity domain of the cusp analogy may be severely restricted according to the parameters of a given experiment, as Fig. 8 shows. When the asymptotic shape is attained, the power law $h/x_r = [(x - x_{cl})/x_r]^{3/2}$ is approached, but it is soon perturbed by the decrease of Ca. Instead, in the experiment reported in Fig. 5, Ca remains well above unity for a considerable time, so that the asymptotic stage is well developed.

In summary, there exists an asymptotic stage during which the roll-like head of a viscous gravity current with Ca$>1$ exhibits an invariant shape, whose lower part may be considered as half a cusped entrance of the free surface. This result relates apparently different phenomena, such as the appearance of a 180° dynamic contact angle for viscous spreadings with Ca$\gg 1$ and the formation of cusped entrances in the free surface of Stokes flows.


[1] B. M. Marino, L. Thomas, J. Diez, and R. Gratton, J. Colloid Interface Sci. **177**, 14 (1996).

[2] S. Betelú, J. A. Diez, L. P. Thomas, R. Gratton, and B. M. Marino, J. Numer. Methods Fluids (to be published).

[3] R. L. Hoffman, J. Colloid Interface Sci. **50**, 228 (1975).

[4] C. G. Ngan and E. B. Dusan, J. Fluid Mech. **118**, 27 (1982).

[5] P. D. de Gennes, Rev. Mod. Phys. **57**, 827 (1985).

[6] J. D. Chen, J. Colloid Interface Sci. **122**, 60 (1988).

[7] C. Huh and L. E. Scriven, J. Colloid Interface Sci. **35**, 85 (1988).

[8] L. M. Hocking, Q. J. Mech. Appl. Math. **34**, 37 (1981); L. M. Hocking and A. D. Rivers, J. Fluid Mech. **121**, 425 (1982); L. M. Hocking, Q. J. Mech. Appl. Math. **36**, 55 (1983).

[9] E. B. Dussan, Annu. Rev. Mech. **11**, 371 (1979).

[10] L. Leger and J. F. Joanny, Rep. Prog. Phys. 431 (1992).

[11] J. A. Diez, R. Gratton, L. P. Thomas, and B. Marino, J. Colloid Interface Sci. **106**, 15 (1994); J. A. Diez, R. Gratton, L. P. Thomas, and B. Marino, Phys. Fluids **6**, 24 (1994); R. Gratton, J. A. Diez, L. P. Thomas, B. Marino, and S. Betelú, Phys. Rev. E **53**, 3563 (1996).

[12] D. D. Joseph *et al.*, J. Fluid Mech. **223**, 383 (1991).

[13] J. T. Jeong and H. K. Moffatt, J. Fluid Mech. **241**, 1 (1992).

[14] L. K. Antanovskii, Eur. J. Mech. B **13**, 491 (1994).

[15] Y. J. Liu, T. Y. Liao, and D. D. Joseph, J. Fluid Mech. **304**, 321 (1995).

[16] D. D. Joseph, J. Non-Newtonian Fluid Mech. **44**, 127 (1992).

[17] D. G. Aronson, SIAM J. Appl. Math. **19**, 299 (1970).

[18] A. A. Lacey, J. R. Ockendon, and A. B. Tayler, J. Appl. Math. **42**, 1252 (1982).

[19] W. L. Kath and D. S. Cohen, Stud. Appl. Math. **67**, 79 (1982).

[20] B. M. Marino, L. P. Thomas, R. Gratton, J. A. Diez, S. Betelu, and J. Gratton, Phys. Rev. E **54**, 2623 (1996).

[21] H. A. Barnes, J. F. Fulton, and K. Walters, *An Introduction to Rheology* (Elsevier, New York, 1989).

[22] R. R. Rahalker *et al.*, Proc. R. Soc. London, Ser. A **394**, 207 (1984).

[23] L. P. Thomas, B. M. Marino, and R. Gratton, Phys. Rev. Lett. **78**, 654 (1997).

[24] L. P. Thomas, R. Gratton, and B. M. Marino, Appl. Opt. (to be published).

[25] H. E. Huppert, J. Fluid Mech. **121**, 43 (1982).